



High-order doubly asymptotic absorbing boundaries for the acoustic wave equation

Carolin Birk (1), Suriyon Prempramote (2) and Chongmin Song (2)

(1) Institut für Statik und Dynamik der Tragwerke, Technische Universität Dresden, 01062 Dresden, Germany
(2) School of Civil and Environmental Engineering, University of New South Wales, Sydney NSW 2052, Australia

PACS: 43.10.Ce, 43.20.Mv, 43.20.Px

ABSTRACT

This paper is devoted to the numerical modelling of transient exterior acoustics problems. The propagation of acoustic waves in waveguides is addressed. These systems can be decoupled into a series of scalar problems using the method of separation of variables. For each mode, high-order doubly asymptotic boundaries for the resulting scalar wave equation are proposed. This is based on a continued-fraction solution of the frequency-dependent modal impedance coefficient, which relates the modal pressure to the modal flux at the near field / far field interface. The continued-fraction solution is transformed into a series of linear equations in the frequency domain by introducing internal variables. This corresponds to a system of first-order differential equations in the time-domain, which fully represents the unbounded waveguide in a transient analysis. Numerical experiments demonstrate that both evanescent and propagating modes can be modelled with high accuracy. This leads to stable time-domain solutions, even for long-time simulations. Highly accurate representations can be achieved for arbitrarily high modes. The proposed method is used to study several transient acoustic wave propagation problems in waveguides.

INTRODUCTION

When modelling wave propagation, it is often necessary to introduce an artificial boundary around the region of interest so that the size of the computational domain is limited to allow the application of well-established numerical methods such as the finite element method. The region exterior to the artificial boundary is regarded as an unbounded domain. A boundary condition mimicking the unbounded domain has to be enforced on the artificial boundary to prevent fictitious reflections that pollute the solution. A direct time-domain formulation is required when non-linearities occur in the region of interest. Such a boundary condition is referred to as ‘absorbing boundary’ in this paper. Extensive literature on various absorbing boundaries exists. Excellent literature reviews can be found in [2, 10, 11, 19, 28].

In theory, an exact absorbing boundary is global in space and time. When a rigorous method (for example the boundary element method [4, 5], the thin-layer method [20] or the scaled boundary finite element method [30]) is employed to construct an absorbing boundary, the formulation is global. The convolution integral and storage of the response history are computationally expensive for large-scale problems and long-time simulations.

As an alternative, a large number of approximate absorbing boundaries have been developed. Well-known examples include the viscous boundary [23], the superposition boundary [25], and the extrapolation boundary [22]. Generally speaking, they are spatially and temporally local, and thus computationally efficient. However, they have to be applied to an artificial boundary sufficiently far away from the region of interest in order to obtain results of acceptable accuracy. This increases the total computational effort.

To increase the accuracy and efficiency of simple absorbing boundaries, high-order local absorbing boundaries have been

proposed. This type of absorbing boundary has the potential of leading to accurate results as the order of approximation increases. At the same time, it is computationally efficient owing to its local formulation. Examples of early developments include the paraxial boundary [6], the Bayliss, Gunzburger and Turkel (BGT) boundary [1] and the multi-direction boundary [18]. The order of derivative in these formulations increases with the order of the absorbing boundary. Beyond the second order, the implementation in a finite element computer program becomes complex and instability may occur.

Researchers in several fields have shown their strong interest in developing absorbing boundaries of arbitrarily high order (see, e.g. [12–16, 21, 27]). Literature reviews are available, for example in Refs. [10, 28]. All the above high-order absorbing boundaries were constructed to absorb propagating waves radiating energy. As they are singly-asymptotic at the high-frequency limit, they are appropriate for radiative fields. In some cases of applications, a part of the total energy may be trapped near the region of interest and may not propagate to infinity. The best-known example is probably the evanescent waves occurring in a waveguide. It is explained in Ref. [17] that inclusion of evanescent modes improves the accuracy of the long-time behaviour of high-order absorbing boundaries.

From an application point of view, it is highly desirable to develop a temporally local absorbing boundary that is capable of accurately mimicking an unbounded domain over the entire frequency range. One advance towards this objective is the introduction of doubly-asymptotic boundaries [7, 8, 29]. This formulation is spatially global as the dynamic stiffness is exact not only at high-frequency limit but also at statics. To the knowledge of the authors, the highest order reported is three [9].

Recently, a new approach to construct temporally local absorbing boundaries of arbitrarily high order has been proposed in

Ref. [3]. It is applicable to both scalar and vector waves. Different from most existing approaches, it seeks a continued fraction solution for the equation of the dynamic stiffness matrix of an unbounded domain obtained using the scaled boundary finite element method [26]. By using the continued fraction solution, the force-displacement relationship of the unbounded domain is formulated as a temporally local absorbing boundary condition in the time domain. However, like other high-order absorbing boundaries, this absorbing boundary is inappropriate to model evanescent waves, and the convergence rate at low frequencies is much lower than at high frequencies.

In this paper, a technique for constructing a high-order doubly asymptotic absorbing boundary is proposed by extending the work in Ref. [3]. The acoustic wave equation in a semi-infinite layer with constant depth (a waveguide) is addressed. The proposed technique can be readily applied to other important problems which can be solved using the method of separation of variables, such as the circular cavity embedded in a full plane and the sphere embedded in full space. The absorbing boundaries derived for these cases can be used directly for the solution of practical problems by introducing straight or circular boundaries. Further work on modelling acoustic problems with more general geometries and inhomogeneities is in progress.

The further outline of this paper is as follows. In the following Section, the governing partial differential equations of the two-dimensional acoustic problem are transformed into a set of ordinary differential equations using the method of separation of variables. A modal impedance coefficient is defined, which relates the amplitude of the modal flux to the amplitude of the modal pressure at the vertical boundary. An algebraic equation for this impedance coefficient as a function of the frequency ω is derived. A high-order absorbing boundary is obtained by expanding the modal impedance coefficient into a doubly asymptotic series of continued fractions. The continued-fraction solution can be expressed as a series of linear equations in the frequency domain [24], which corresponds to a system of first-order differential equations in the time domain. The proposed method is used to study several acoustic wave propagation problems in a waveguide.

MODAL DECOMPOSITION OF ACOUSTIC WAVE EQUATION IN A WAVEGUIDE

Acoustic wave propagation in a semi-infinite two-dimensional layered medium of constant thickness h as shown in Fig. 1 is considered in this paper. In general, the domain is split into a

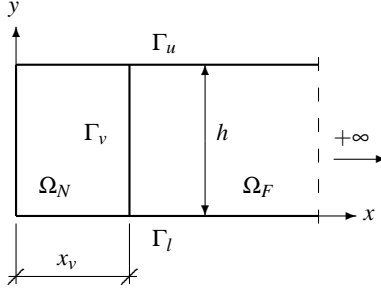


Figure 1: Semi-infinite layer with constant depth h .

rectangular near field region Ω_N and a semi-infinite far field region Ω_F . The two domains are linked by the artificial boundary Γ_v at $x = x_v$. Typically, we are interested in the numerical solution of the acoustic problem in the bounded region Ω_N . This solution can be computed using the well-established finite element method provided that a suitable boundary condition at the artificial boundary Γ_v is available. The aim of this paper is to formulate such an absorbing boundary condition which is

suitable for the analysis of transient acoustics problems. Therefore, we focus on the semi-infinite region Ω_F in the following. The method of separation of variables can be applied to obtain a series of one-dimensional differential equations to describe acoustic wave propagation in Ω_F .

Semi-infinite layer with constant depth

The acoustic wave equation is expressed as,

$$\nabla^2 p = \frac{1}{c^2} \ddot{p}, \quad (1)$$

where $p = p(x, y, t)$ denotes the pressure field and c is the velocity of acoustic wave propagation. At a vertical boundary, the flux $q(x, y, t)$ is defined as

$$q(x, y, t) = p_{,n} = -p_{,x}(x, y, t). \quad (2)$$

It is assumed that a distributed flux q_v is applied to the vertical (artificial) boundary Γ_v .

$$q_v = q(x = x_v, y, t) = -p_{,x}(x = x_v, y, t). \quad (3)$$

Here and in the following, the subscript ‘ v ’ indicates the position x_v . The boundary conditions prescribed at the parallel upper boundary Γ_u and lower boundary Γ_l are satisfied by eigenfunctions using the method of separation of variables. In this paper, the following situation is considered. The lower boundary Γ_l is assumed to be rigid. This corresponds to zero normal flux. At the upper boundary Γ_u , zero pressure is assumed (corresponding to a free water surface, for example).

The pressure field $p = p(x, y, t)$ is written as the product of two functions $\tilde{p} = \tilde{p}(x, t)$ and $Y = Y(y)$,

$$p = \tilde{p}Y. \quad (4)$$

Substituting Eq. (4) in Eq. (1) yields:

$$\tilde{p}_{,xx}Y + \tilde{p}Y_{,yy} = \frac{1}{c^2} \ddot{\tilde{p}}Y. \quad (5)$$

Dividing by $\tilde{p}Y$, Eq. (5) is transformed in two independent differential equations: an ordinary differential equation with respect to the vertical coordinate y (Eq. (6)), and a partial differential equation with respect to x and t (Eq. (7)).

$$-\frac{Y_{,yy}}{Y} = k, \quad (6)$$

$$\frac{\tilde{p}_{,xx}}{\tilde{p}} - \frac{1}{c^2} \frac{\ddot{\tilde{p}}}{\tilde{p}} = k. \quad (7)$$

For convenience, the constant k is chosen as $k = \frac{\lambda^2}{h^2}$. The ordinary differential equation (6) is rewritten as

$$0 = Y_{,yy} + \frac{\lambda^2}{h^2} Y. \quad (8)$$

Its solution is expressed as,

$$Y = C_1 \cos\left(\lambda \frac{y}{h}\right) + C_2 \sin\left(\lambda \frac{y}{h}\right). \quad (9)$$

The integration constants C_1 and C_2 are determined by the boundary conditions at Γ_u and Γ_l . The resulting eigenvalues λ_j and eigenfunctions $Y_j = Y_j(y)$ are summarized in Eq. (10).

$$\left. \begin{array}{l} \cos \lambda = 0, \\ \lambda_j = (2j+1)\frac{\pi}{h}, \quad j = 0, 1, \dots \\ Y_j = \cos\left(\lambda_j \frac{y}{h}\right) \end{array} \right\} \quad \begin{array}{l} \Gamma_l : p_{,y} = 0, \\ \Gamma_u : p = 0 \end{array} \quad (10)$$

The solution of the remaining partial differential equation (7) with respect to x and t for one eigenvalue λ_j is addressed next.

$$\tilde{p}_{j,xx} - \left(\frac{\lambda_j}{h}\right)^2 \tilde{p}_j = \frac{1}{c^2} \ddot{\tilde{p}}_j. \quad (11)$$

Analytical solution

Assuming a time-harmonic behaviour,

$$\tilde{p}_j(x, t) = \tilde{P}_j(x, \omega) e^{i\omega t}, \quad (12)$$

Eq. (11) is re-formulated as:

$$\tilde{P}_{j,xx} - \left(\frac{\lambda_j}{h} \right)^2 \tilde{P}_j = -\frac{\omega^2}{c^2} \tilde{P}_j, \quad (13)$$

where the symbol \tilde{P}_j denotes the amplitude of the modal pressure \tilde{p}_j . Using the dimensionless parameter a with,

$$a = \omega \frac{h}{c}, \quad (14)$$

the solution of Eq. (13) leading to a finite modal pressure at $x \rightarrow \infty$ is expressed as,

$$\tilde{P}_j = C \cdot e^{-\sqrt{\lambda_j^2 - a^2} \frac{x}{h}}. \quad (15)$$

For the semi-infinite layer extending to the right-hand side, the amplitude $Q(x, y, \omega)$ of the flux $q(x, y, t)$,

$$q(x, y, t) = Q(x, y, \omega) e^{i\omega t}, \quad (16)$$

as defined in Eq. (2) is expressed after modal decomposition of the pressure field as

$$Q(x, y, \omega) = - \sum_{j=0}^{\infty} (\tilde{P}_j(x, \omega))_{,x} Y_j(y). \quad (17)$$

A modal flux-temperature relationship, which is independent of y , is obtained by making use of the orthogonality of the eigenfunctions Y_j . Multiplying Eq. (17) by Y_j and integrating over the depth of the layer we obtain for one mode j ,

$$\int_{y=0}^h Q(x, y, \omega) Y_j(y) dy = -\frac{h}{2} (\tilde{P}_j(x, \omega))_{,x}. \quad (18)$$

The symbol $\tilde{R}_j = \tilde{R}_j(x, \omega)$ is introduced to denote the modal flux at a vertical boundary:

$$\tilde{R}_j(x, \omega) = 2 \int_{y=0}^h Q(x, y, \omega) Y_j(y) dy. \quad (19)$$

Equation (20) follows from Eqs. (18) and (19) as,

$$\tilde{R}_j = -h \tilde{P}_{j,x}, \quad (20)$$

with,

$$\tilde{P}_{j,x} = -\sqrt{\lambda_j^2 - a^2} \frac{1}{h} C \cdot e^{-\sqrt{\lambda_j^2 - a^2} \frac{x}{h}} = -\sqrt{\lambda_j^2 - a^2} \frac{1}{h} \tilde{P}_j. \quad (21)$$

On the other hand, at the vertical boundary Γ_v the amplitude of the modal flux $\tilde{R}_j(x_v)$ is related to the amplitude of the modal pressure $\tilde{P}_j(x_v)$ through:

$$\tilde{R}_j(x_v, a) = S(a) \tilde{P}_j(x_v, a). \quad (22)$$

The flux-pressure relationship is characterized by the coefficient $S(a)$, which is a function of the dimensionless parameter a and thus of the frequency ω . It is referred to as *impedance coefficient* in the following. Evaluating Eq. (21) at $x = x_v$ and equating Eqs. (20) and (22), the modal impedance coefficient of the semi-infinite layer is obtained as:

$$S(a) = \sqrt{\lambda_j^2 - a^2}. \quad (23)$$

Eqs. (22) and (23) form the analytical solution in the frequency domain.

To obtain a reference solution to validate numerical results in the time domain, the response to a unit-impulse modal flux $\tilde{r}_{jl}(x_v, t) = \delta(t)$ applied at $x = x_v$ is evaluated. The Fourier transform of the unit-impulse function is $\tilde{R}_{jl}(x_v) = 1$. The amplitude $\tilde{P}_{jl}(x_v)$ of the modal pressure due to the above unit-impulse modal flux $\tilde{r}_{jl}(x_v)$ follows from Eqs. (22) and (23):

$$\tilde{P}_{jl}(x_v) = \frac{1}{\sqrt{\lambda_j^2 - a^2}}. \quad (24)$$

The unit-impulse response $\tilde{p}_{jl}(x_v)$ in the time domain is obtained by applying the inverse Fourier transformation to Eq. (24). For $\tilde{P}_{jl}(x_v)$ given in Eq. (24), the Fourier integral can be evaluated in closed form,

$$\tilde{p}_{jl}(x_v, t) = \frac{c}{h} J_0 \left(\lambda_j \frac{ct}{h} \right) H(t) \quad (25)$$

with the dimensionless time,

$$\bar{t} = \frac{ct}{h}. \quad (26)$$

The symbols J_0 and $H(t)$ denote the zero order first kind Bessel function and the Heaviside step function, respectively.

The pressure response due to an arbitrary prescribed modal flux $\tilde{r}_j(x_v, t)$ can finally be expressed as a convolution integral,

$$\tilde{p}_j(x_v, t) = \int_0^t \tilde{p}_{jl}(x_v, t - \tau) \tilde{r}_j(x_v, \tau) d\tau. \quad (27)$$

The numerical evaluation of the convolution integral in Eq. (27) can be computationally expensive for longer observation times and is not desired in a general time-domain analysis. In order to derive a local formulation, the problem is recast in terms of the modal impedance coefficient $S(a)$ in the following.

Formulation in terms of modal impedance coefficient

An equation for the modal impedance coefficient is obtained rewriting Eq. (23) as:

$$S^2 = \lambda_j^2 - a^2 = \lambda^2 + (ia)^2. \quad (28)$$

Eq. (28) can be solved by expanding $S(a)$ into a doubly asymptotic series of continued fractions in terms of ia . Following the procedure described in Ref. [24], the coefficients of the continued-fraction expansion are obtained as functions of the eigenvalue λ_j . Thus, a different continued-fraction representation is constructed for each mode j . This is avoided normalizing both the impedance coefficient S and the dimensionless frequency a with respect to the eigenvalue λ_j ,

$$\bar{S} = \frac{S}{\lambda_j}, \quad \bar{a} = \frac{a}{\lambda_j}, \quad (29)$$

Using Eq. (29), Eq. (28) is rewritten as,

$$\bar{S}^2 = 1 - \bar{a}^2. \quad (30)$$

DOUBLY ASYMPTOTIC EXPANSION OF MODAL IMPEDANCE COEFFICIENT

The continued-fraction solution of Eq. (30) is demonstrated in the following. The procedure is analogous to the derivation presented in Ref. [24], but differs in that only one and the same continued-fraction expansion is obtained for all modes of the semi-infinite layer. In a first step, an asymptotic expansion of the normalized impedance coefficient valid for high values $\bar{a} \rightarrow \infty$ is constructed analogous to Ref. [3].

Asymptotic expansion for $\bar{a} \rightarrow \infty$

For high values $\bar{a} \rightarrow \infty$, the normalized impedance coefficient \bar{S} tends to $i\bar{a}$. This can easily be verified considering Eq. (30). For arbitrary values \bar{a} , the normalized impedance coefficient is expressed as:

$$\bar{S} = i\bar{a} - \left(Y^{(1)}(\bar{a}) \right)^{-1}. \quad (31)$$

In Eq. (31) the term $\left(Y^{(1)}(\bar{a}) \right)^{-1}$ represents the residual of the asymptotic expansion, i. e. the difference between the normalized impedance coefficient and its value for $\bar{a} \rightarrow \infty$. The residual tends to zero for $\bar{a} \rightarrow \infty$. For convenience, it is expressed as the inverse of a yet unknown function $Y^{(1)}(\bar{a})$ of \bar{a} . The superscript (1) indicates the first step of a recursive procedure, as will become evident further in the derivation. Substituting Eq. (31) in Eq. (30) results in:

$$-1 - 2i\bar{a} \left(Y^{(1)}(\bar{a}) \right)^{-1} + \left(Y^{(1)}(\bar{a}) \right)^{-2} = 0. \quad (32)$$

Eq. (32) can be written as the $i = 1$ case of:

$$1 - 2b^{(i)}i\bar{a}Y^{(i)}(\bar{a}) - \left(Y^{(i)}(\bar{a}) \right)^2 = 0, \quad (33)$$

with

$$b^{(1)} = 1. \quad (34)$$

Analogous to Eq. (31), the unknown function $Y^{(i)}(\bar{a})$ is decomposed as:

$$Y^{(i)}(\bar{a}) = i\bar{a}C^{(i)} - \left(Y^{(i+1)}(\bar{a}) \right)^{-1}. \quad (35)$$

Here, we assume that $Y^{(i)}(\bar{a})$ tends to a linear function of $i\bar{a}$ for $\bar{a} \rightarrow \infty$. The slope $C^{(i)}$ of this linear function is yet unknown. Substituting Eq. (35) in Eq. (33) yields:

$$-(i\bar{a})^2 \left(\left(C^{(i)} \right)^2 + 2b^{(i)}C^{(i)} \right) + 1 + 2i\bar{a} \left(C^{(i)} + b^{(i)} \right) \times \left(Y^{(i+1)}(\bar{a}) \right)^{-1} - \left(Y^{(i+1)}(\bar{a}) \right)^{-2} = 0. \quad (36)$$

This is an equation for the coefficient $C^{(i)}$ and for the yet unknown residual $\left(Y^{(i+1)}(\bar{a}) \right)^{-1}$. Individual equations are obtained by setting terms corresponding to different powers of $i\bar{a}$ to zero in descending order. Setting the first term of Eq. (36) (i. e. $(i\bar{a})^2$) to zero yields an equation for $C^{(i)}$,

$$C^{(i)} = -2b^{(i)}, \quad (37)$$

For $i = 1$ we obtain $C^{(1)} = -2$. Setting the remainder of Eq. (36) to zero using Eq. (37) leads to an equation for $Y^{(i+1)}(\bar{a})$,

$$1 + 2i\bar{a}b^{(i)}Y^{(i+1)}(\bar{a}) - \left(Y^{(i+1)}(\bar{a}) \right)^2 = 0. \quad (38)$$

The recursive formula

$$b^{(i+1)} = -b^{(i)}, \quad (39)$$

is introduced to update the coefficient b . Using Eq. (39), Eq. (38) can be written as

$$1 - 2i\bar{a}b^{(i+1)}Y^{(i+1)}(\bar{a}) - \left(Y^{(i+1)}(\bar{a}) \right)^2 = 0. \quad (40)$$

This is the $(i+1)$ case of Eq. (33). General equations for $b^{(i)}$ and $C^{(i)}$ follow from Eqs. (34), (39) and (37) as:

$$b^{(i)} = (-1)^{i+1}, \quad i = 1, 2, \dots, M_H, \quad (41)$$

$$C^{(i)} = (-1)^i 2, \quad i = 1, 2, \dots, M_H. \quad (42)$$

After $i = M_H$ steps, the normalized impedance coefficient is expressed as

$$\bar{S} = i\bar{a} - \frac{1}{C^{(1)}(i\bar{a}) - \frac{1}{C^{(2)}(i\bar{a}) - \dots - \frac{1}{C^{(M_H)}(i\bar{a}) - \left(Y^{(M_H+1)}(\bar{a}) \right)^{-1}}}} \quad (43)$$

For a given order M_H , the coefficients $C^{(i)}$, ($i = 1 \dots M_H$) of this continued-fraction expansion can be calculated using Eq. (42). The remaining residual $\left(Y^{(M_H+1)}(\bar{a}) \right)^{-1}$ is yet unknown. In order to find a solution which is valid over the whole range of \bar{a} , the remaining residual term $\left(Y^{(M_H+1)}(\bar{a}) \right)^{-1}$ is determined such that the final doubly asymptotic expansion of $\bar{S}(\bar{a})$ is exact for $\bar{a} = 0$.

Asymptotic expansion for $\bar{a} \rightarrow 0$

The inverse $Y^{(M_H+1)}(\bar{a})$ of the residual term corresponding to a continued-fraction expansion for high values $\bar{a} \rightarrow \infty$ of degree M_H is denoted as:

$$Y^{(M_H+1)}(\bar{a}) = Y_L(\bar{a}). \quad (44)$$

Using Eq. (44), the $i = M_H + 1$ case of Eq. (33) is written as:

$$1 - 2i\bar{a}b_L Y_L(\bar{a}) - (Y_L(\bar{a}))^2 = 0, \quad (45)$$

with

$$b_L = b^{(M_H+1)} = (-1)^{M_H}. \quad (46)$$

The unknown function $Y_L(\bar{a})$ is expanded as:

$$Y_L(\bar{a}) = K_L^{(0)} + i\bar{a}C_L^{(0)} - (i\bar{a})^2 \left(Y_L^{(1)}(\bar{a}) \right)^{-1}. \quad (47)$$

This expansion is designed such that $Y_L(\bar{a})$ approaches the constant $K_L^{(0)}$ for $\bar{a} \rightarrow 0$, whereas the yet undetermined linear term $i\bar{a}C_L^{(0)}$ and the residual $(i\bar{a})^2 \left(Y_L^{(1)}(\bar{a}) \right)^{-1}$ vanish. Substituting Eq. (47) in Eq. (45) yields:

$$1 - \left(K_L^{(0)} \right)^2 - i\bar{a} \left(2b_L K_L^{(0)} + 2K_L^{(0)} C_L^{(0)} \right) + (i\bar{a})^2 \left(-2b_L C_L^{(0)} - \left(C_L^{(0)} \right)^2 + 2 \left(K_L^{(0)} + i\bar{a} \left(C_L^{(0)} + b_L \right) \right) \times \left(Y_L^{(1)}(\bar{a}) \right)^{-1} - (i\bar{a})^2 \left(Y_L^{(1)}(\bar{a}) \right)^{-2} \right). \quad (48)$$

Equations for $K_L^{(0)}$, $C_L^{(0)}$ and $\left(Y_L^{(1)}(\bar{a}) \right)^{-1}$ are found by setting terms corresponding to different powers of $(i\bar{a})$ to zero in ascending order. The constant term (i. e. $(i\bar{a})^0$) yields:

$$1 - \left(K_L^{(0)} \right)^2 = 0. \quad (49)$$

Eq. (49) has two possible solutions. The one leading to the correct normalized impedance for $\bar{a} = 0$, $\bar{S}(\bar{a} = 0) = 1$, should be chosen. This is:

$$K_L^{(0)} = (-1)^{M_H+1}. \quad (50)$$

Note that the sign of $K_L^{(0)}$ depends on the order of continued-fraction expansion M_H for high values of \bar{a} . The linear term in Eq. (48) leads to an equation for $C_L^{(0)}$:

$$C_L^{(0)} = -b_L = (-1)^{M_H+1}. \quad (51)$$

The remaining term in Eq. (48) yields an equation for the unknown function $Y_L^{(1)}(\bar{a})$.

$$(i\bar{a})^2 - 2 \left(K_L^{(0)} + i\bar{a} \left(C_L^{(0)} + b_L \right) \right) Y_L^{(1)}(\bar{a}) + \left(2b_L C_L^{(0)} + \left(C_L^{(0)} \right)^2 \right) \left(Y_L^{(1)}(\bar{a}) \right)^2 = 0. \quad (52)$$

Using Eqs. (50) and (51), Eq. (52) can be written as the $i = 1$ case of:

$$(i\bar{a})^2 - 2b_L^{(i)} Y_L^{(i)}(\bar{a}) - \left(Y_L^{(i)}(\bar{a}) \right)^2 = 0, \quad (53)$$

with

$$b_L^{(1)} = -b_L = (-1)^{M_H+1}. \quad (54)$$

Analogous to Eq. (47) the unknown function $Y_L^{(i)}(\bar{a})$ is decomposed as:

$$Y_L^{(i)}(\bar{a}) = K_L^{(i)} - (i\bar{a})^2 \left(Y_L^{(i+1)}(\bar{a}) \right)^{-1}. \quad (55)$$

Note that the linear term is omitted in Eq. (55) as its solution is equal to zero, which can easily be verified. Substituting Eq. (55) into Eq. (53) leads to:

$$- \left(2b_L^{(i)} K_L^{(i)} + \left(K_L^{(i)} \right)^2 \right) + (i\bar{a})^2 \left(1 + 2 \left(b_L^{(i)} + K_L^{(i)} \right) \times \left(Y_L^{(i+1)}(\bar{a}) \right)^{-1} - (i\bar{a})^2 \left(Y_L^{(i+1)}(\bar{a}) \right)^{-2} \right) = 0. \quad (56)$$

In the recursive procedure, general expressions for the coefficients $K_L^{(i)}$ and for the unknown function $Y_L^{(i+1)}(\bar{a})$ are determined setting the terms corresponding to different powers of $(i\bar{a})$ equal to zero in ascending order. Setting the constant term equal to zero yields for $K_L^{(i)}$:

$$K_L^{(i)} = -2b_L^{(i)}. \quad (57)$$

Setting the remaining term to zero and using Eq. (57) leads to:

$$(i\bar{a})^2 + 2b_L^{(i)} Y_L^{(i+1)}(\bar{a}) - \left(Y_L^{(i+1)}(\bar{a}) \right)^2 = 0. \quad (58)$$

Eq. (58) is the case $(i+1)$ of Eq. (53) with

$$b_L^{(i+1)} = -b_L^{(i)}. \quad (59)$$

Using Eq. (54), the constants $b_L^{(i)}$ and $K_L^{(i)}$ can be explicitly expressed as:

$$b_L^{(i)} = (-1)^{M_H+i}, \quad i = 1, 2, \dots, M_L, \quad (60)$$

$$K_L^{(i)} = 2(-1)^{M_H+i+1}, \quad i = 1, 2, \dots, M_L. \quad (61)$$

The recursive procedure is terminated with the assumption

$$\left(Y_L^{(M_L+1)}(\bar{a}) \right)^{-1} = 0. \quad (62)$$

The doubly asymptotic continued fraction solution is constructed by combining the asymptotic expansion for $\bar{a} \rightarrow \infty$ with the solution for $\bar{a} \rightarrow 0$. For example, the order $M_H = M_L = 2$ doubly asymptotic continued fraction solution is obtained as

$$\bar{S}(\bar{a}) = i\bar{a} - \frac{1}{-2(i\bar{a}) - \frac{1}{2(i\bar{a}) - \frac{1}{-1-i\bar{a} - \frac{(i\bar{a})^2}{2 - \frac{(i\bar{a})^2}{-2}}}}}. \quad (63)$$

In the following, a time-domain model for acoustic wave propagation in a semi-infinite layer is obtained by transforming the continued-fraction solution into a system of linear equations in terms of $i\omega$. This is done by introducing internal variables. The proposed method can be extended to the multidimensional case straightforwardly.

IMPLEMENTATION IN THE TIME DOMAIN

In order to derive a time-domain equivalent of the doubly asymptotic continued-fraction expansion of the normalized impedance coefficient, the equations derived above are re-assembled, starting with Eqs. (22), (29) and (31):

$$\tilde{R}_j(x_v) = S\tilde{P}_j(x_v) = \lambda_j \tilde{S}\tilde{P}_j(x_v) = \left(\lambda_j i\bar{a} - \lambda_j \left(Y^{(1)}(\bar{a}) \right)^{-1} \right) \tilde{P}_j(x_v). \quad (64)$$

Using $\bar{a} = a/\lambda_j$ and introducing an internal variable $\tilde{P}_j^{(1)}$, a first linear equation (65) in terms of ia is obtained.

$$\tilde{R}_j(x_v) = ia\tilde{P}_j(x_v) - \lambda_j \tilde{P}_j^{(1)}, \quad (65)$$

with

$$\tilde{P}_j(x_v) = Y^{(1)}(\bar{a}) \tilde{P}_j^{(1)}. \quad (66)$$

Using Eq. (35), Eq. (66) can be written as:

$$\tilde{P}_j(x_v) = \left(iaC^{(1)} - \left(Y^{(2)}(\bar{a}) \right)^{-1} \right) \tilde{P}_j^{(1)}. \quad (67)$$

A second linear equation (68) in terms of ia is obtained introducing a second internal variable $\tilde{P}_j^{(2)}$.

$$\lambda_j \tilde{P}_j(x_v) = iaC^{(1)} \tilde{P}_j^{(1)} - \lambda_j \tilde{P}_j^{(2)} \quad (68)$$

This process is continued until a total of M_H internal variables have been introduced to represent the high-asymptotic part of the continued-fraction expansion. The $(M_H + 1)$ -th linear equation in terms of ia can be written as:

$$\lambda_j \tilde{P}_j^{(M_H-1)} = iaC^{(M_H)} \tilde{P}_j^{(M_H)} - \lambda_j \tilde{P}_j^{(M_H+1)}. \quad (69)$$

The internal variable $\tilde{P}_j^{(M_H+1)}$ is defined as:

$$\tilde{P}_j^{(M_H)} = Y^{(M_H+1)}(\bar{a}) \tilde{P}_j^{(M_H+1)} = Y_L(\bar{a}) \tilde{P}_j^{(M_H+1)}, \quad (70)$$

with the residual $Y^{(M_H+1)}$ given in Eq. (44). Using Eq. (47), Eq. (70) can be written as:

$$\tilde{P}_j^{(M_H)} = \left(K_L^{(0)} + i\bar{a}C_L^{(0)} - (i\bar{a})^2 \left(Y_L^{(1)}(\bar{a}) \right)^{-1} \right) \tilde{P}_j^{(M_H+1)}. \quad (71)$$

The $(M_H + 2)$ -th linear equation (72) in terms of ia follows by introducing the internal variable $\tilde{P}_{jL}^{(1)}$ as defined in Eq. (73).

$$\lambda_j \tilde{P}_j^{(M_H)} = \left(\lambda_j K_L^{(0)} + iaC_L^{(0)} \right) \tilde{P}_j^{(M_H+1)} - ia\tilde{P}_{jL}^{(1)}. \quad (72)$$

$$ia \left(Y_L^{(1)}(\bar{a}) \right)^{-1} \tilde{P}_j^{(M_H+1)} = \tilde{P}_{jL}^{(1)}. \quad (73)$$

Using Eq. (55), Eq. (73) can be reformulated as:

$$ia\tilde{P}_j^{(M_H+1)} = \lambda_j K_L^{(1)} \tilde{P}_{jL}^{(1)} - ia\tilde{P}_{jL}^{(2)}, \quad (74)$$

with

$$ia\tilde{P}_{jL}^{(1)} = \lambda_j Y_L^{(2)}(\bar{a}) \tilde{P}_{jL}^{(2)}. \quad (75)$$

This procedure is continued until a total of M_L internal variables $\tilde{P}_{jL}^{(i)}$, ($i = 1, \dots, M_L$) have been introduced to represent the low-asymptotic part of the continued-fraction expansion. The process terminates with the assumption $Y_L^{(M_L+1)} = 0$. The final, $(M_H + M_L + 2)$ -th linear equation (76) in terms of ia is:

$$ia\tilde{P}_{jL}^{(M_L-1)} = \lambda_j K_L^{(M_L)} \tilde{P}_{jL}^{(M_L)}. \quad (76)$$

The linear equations (65), (68)–(69), (72), (74)–(76) can be summarized in matrix form:

$$(\lambda_j[K] + ia[C]) \{Z\} = \{F\}, \quad (77)$$

with

$$\{Z\} = \begin{bmatrix} \tilde{P}_j(x_v) & \tilde{P}_j^{(1)} & \dots & \tilde{P}_j^{(M_H)} & \tilde{P}_j^{(M_H+1)} \\ & \tilde{P}_{jL}^{(1)} & \dots & \tilde{P}_{jL}^{(M_L)} \end{bmatrix}^T, \quad (78)$$

$$\{F\} = [\tilde{R}_j(x_v) \ 0 \ \dots \ 0 \ 0 \ 0 \ \dots \ 0]^T, \quad (79)$$

$$[K] = \begin{bmatrix} 0 & -1 & & & & & \\ -1 & 0 & \ddots & & & & \\ \ddots & \ddots & -1 & & & & \\ & -1 & 0 & -1 & & & \\ & & -1 & K_L^{(0)} & 0 & & \\ & & & 0 & K_L^{(1)} & \ddots & \\ & & & & \ddots & \ddots & 0 \\ & & & & & 0 & K_L^{(M_L)} \end{bmatrix}, \quad (80)$$

$$[C] = \begin{bmatrix} 1 & 0 & & & & & \\ 0 & C^{(1)} & \ddots & & & & \\ \ddots & \ddots & 0 & & & & \\ & 0 & C^{(M_H)} & 0 & & & \\ & & 0 & C_L^{(0)} & -1 & & \\ & & & -1 & 0 & \ddots & \\ & & & & \ddots & \ddots & -1 \\ & & & & & -1 & 0 \end{bmatrix}. \quad (81)$$

Eq. (77) is the flux-pressure relationship for one mode λ_j formulated in terms of ia . Note that the matrices $[K]$ and $[C]$ do not depend on the eigenvalue λ_j . A formulation in terms of the frequency ω is obtained using Eq. (14):

$$\left(\lambda_j[K] + i\omega \frac{h}{c}[C] \right) \{Z\} = \{F\}. \quad (82)$$

Eq. (82) in the frequency domain corresponds to the following system of first-order differential equations in the time domain:

$$\lambda_j[K] \{z(t)\} + \frac{h}{c}[C] \{\dot{z}(t)\} = \{f(t)\}. \quad (83)$$

Eq. (83) represents the modal flux-pressure relationship of the waveguide in the time-domain. The vector $\{z(t)\}$ contains the unknown, time-dependent modal pressure $\tilde{p}_j(x_v, t)$ at the near field / far field interface and the corresponding time-dependent internal variables $\tilde{p}_j^{(1)}(t), \dots, \tilde{p}_j^{(M_H+1)}(t), \tilde{p}_{jL}^{(1)}(t) \dots \tilde{p}_{jL}^{(M_L)}(t)$. The right-hand side vector $\{f(t)\}$ contains the time-dependent modal flux $\tilde{r}_j(x_v, t)$ at $x = x_v$.

NUMERICAL EXAMPLES

Single mode of the waveguide

A single mode λ_j of the semi-infinite layer is considered. The normalized modal impedance coefficient \bar{S} is shown in Fig. 2 as a function of the dimensionless frequency a for values ranging from zero to $3\lambda_j$. In Fig. 2, the point $a/\lambda_j = 1$ corresponds to the cutoff frequency. It can be seen that the doubly-asymptotic expansion of degree $M_H = M_L = 2$ agrees very well with the corresponding analytical solution. Slight deviations occur in

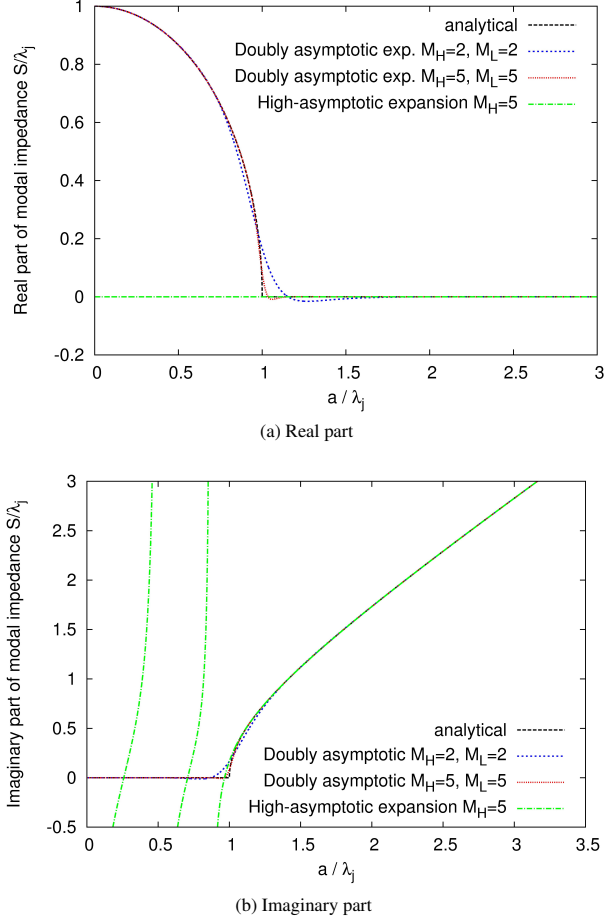


Figure 2: Normalized modal impedance coefficient \bar{S} of semi-infinite layer as a function of the dimensionless frequency a

the vicinity of $a/\lambda_j = 1$. This can be improved by increasing the degree of expansion, as can be seen for $M_H = M_L = 5$. The corresponding high-asymptotic expansion is also shown for $M_H = 5$. Above the characteristic point $a/\lambda_j = 1.0$ a very good agreement, comparable to that of the doubly asymptotic expansion of degree $M_H = M_L = 2$, is achieved using the high-asymptotic expansion. However, for values below $a/\lambda_j = 1.0$ the imaginary part of the high-asymptotic expansion diverges. Its real part is always zero, as is expected. Fig. 2 illustrates that the high-frequency asymptotic expansion of Ref. [3] fails when wave propagation in a semi-infinite layer is modelled.

The modal temperature response to a unit-impulse modal flux is computed using the proposed procedure. The normalized impedance coefficient $\bar{S}(\bar{a})$ is expanded into a doubly asymptotic series of continued fractions as described above. The degrees M_H and M_L of the two expansions for high and low values of \bar{a} , respectively, are chosen as $M_H = M_L = 2$ and $M_H = M_L = 5$, respectively. The computed normalized modal pressure $\tilde{p}_j(x_v, t)h/c$ is compared to the analytical solution given in Eq. (25) in Fig. 3.

It can be seen in Fig. 3a, that the low-order doubly asymptotic absorbing boundary ($M_H = M_L = 2$) is very accurate for the first two periods ($\lambda_j \bar{t} < 10$). After that, the unit-impulse response is underestimated. The accuracy of the doubly-asymptotic absorbing boundary increases rapidly as its order increases. This is demonstrated in Fig. 3b. For $M_H = M_L = 5$, very good agreement with the exact solution is obtained for the first 10 periods. The doubly-asymptotic absorbing boundary is significantly more accurate at late time than a corresponding singly-asymptotic absorbing boundary with the same number of inter-

nal variables. No ‘fictitious reflections’ occur.

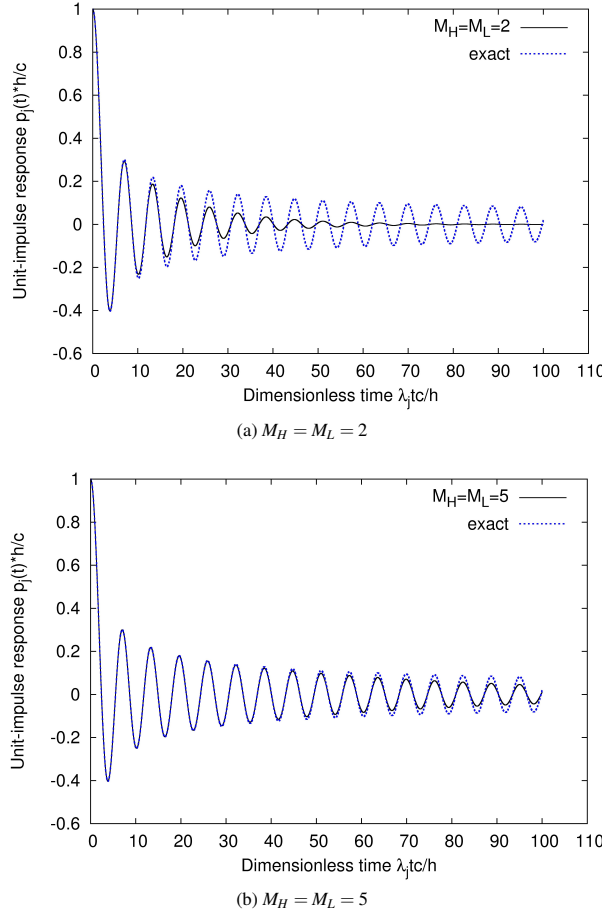


Figure 3: Normalized modal pressure $\tilde{p}_j(t)$ at $x = x_v$ due to unit-impulse modal flux r_{jl} applied at $x = x_v$, $t = 0$.

Two-dimensional analysis

In a truly two-dimensional analysis, the pressure field $p(x = x_v, y, t)$ due to an arbitrary given flux $q(x = x_v, y, t)$ at $x = x_v$ is obtained by modal superposition.

$$p(x = x_v, y, t) = \sum_{j=0}^{\infty} \tilde{p}_j(x_v, t) Y_j(y). \quad (84)$$

The time-dependent modal pressure $\tilde{p}_j(x_v, t)$ is calculated directly in the time-domain using standard time-stepping schemes. For each mode j , the right hand-side vector $\{f(t)\}$ in Eq. (83) contains the corresponding time-dependent modal flux $\tilde{r}_j(x_v, t)$, which is obtained evaluating Eq. (19) at $x = x_v$.

$$\{f(t)\} = [\tilde{r}_j(x_v, t) \quad 0 \quad \cdots \quad 0]^T, \quad (85)$$

$$\tilde{r}_j(x_v, t) = 2 \int_0^h q_v(y, t) Y_j(y) dy. \quad (86)$$

A two-dimensional reservoir of depth $h = 130\text{m}$ is considered. The velocity of wave propagation c and mass density ρ of water are given as

$$c = 1440\text{m/s}, \quad \rho = 1000\text{kg/m}^3. \quad (87)$$

The reservoir is assumed to be bounded by a rigid dam at the vertical boundary Γ_v . A uniform unit-impulse horizontal acceleration,

$$a_x = \hat{a}_x \delta(t - t_0), \quad \hat{a}_x = 1.0 \frac{m}{s^2}, \quad (88)$$

is applied to the rigid dam at $t_0 = 0\text{s}$. This acceleration corresponds to the prescribed flux $q_v(y, t)$ given in Eq. (89):

$$q_v(y, t) = Q_v \delta(t - t_0) = -a_x \rho \delta(t - t_0). \quad (89)$$

An analytical solution for the resulting pressure distribution at $x = x_v$ is constructed superimposing the modal unit-step response given in Eq. (25) of all modes λ_j :

$$p(x_v, y, t) = -2\rho \hat{a}_x c \sum_{j=0}^{\infty} \frac{(-1)^j}{\lambda_j} J_0\left(\lambda_j \frac{ct}{h}\right) \cos\left(\lambda_j \frac{y}{h}\right). \quad (90)$$

A comparison between the time-dependent pressure at the reservoir bottom ($x = x_v, y = 0$) computed using the presented approach with $M_H = M_L = 2, M_H = M_L = 5$ and the corresponding analytical solution is shown in Fig. 4. Only the first 10 modes have been taken into account. The solution using 20 modes is very close to the curves displayed in Fig. 4 and not shown here for clarity. As for the single mode, the agreement

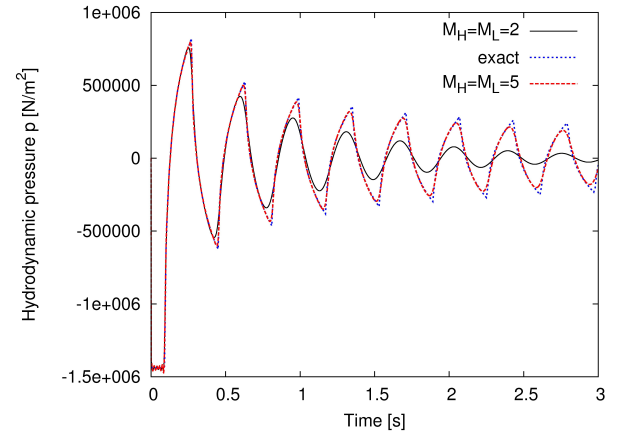


Figure 4: Hydrodynamic pressure at reservoir bottom ($x = x_v, z = 0$) due to $a_x = 1.0\text{m/s}^2 \delta(t - t_0)$, $t_0 = 0$. 10 modes. Time step: $\Delta t = 0.001\text{s}$.

between the analytical solution and the proposed approach with $M_H = M_L = 2$ is good for the first period, whereas the late time response is underestimated using a low-order expansion. This is improved using a high-order doubly asymptotic expansion. The result obtained using $M_H = M_L = 5$ agrees very well with the analytical solution. This confirms the high accuracy of the proposed high-order absorbing boundary for acoustic wave propagation.

Although only impulse functions have been considered here, the proposed model can be used to simulate the time-dependent distribution of the unknown pressure $p(x_v, y, t)$ due to arbitrary transient boundary conditions $q_v(t)$.

CONCLUSIONS

A novel approach for constructing high-order doubly asymptotic absorbing boundaries of arbitrary order has been proposed. The derivation and implementation are presented for the transient analysis of acoustic waves travelling in a waveguide. The modal impedance of the proposed doubly asymptotic absorbing boundary converges rapidly to the exact solution in the frequency-domain as its order increases. Evanescent waves and late-time (low-frequency) responses are simulated accurately. The doubly asymptotic absorbing boundary shows significant improvement in accuracy in comparison with the singly asymptotic absorbing boundary with the same number of terms.

The high-order doubly asymptotic absorbing boundaries are expressed as first-order ordinary differential equations in time.

The two time-dependent coefficient matrices are symmetric and tri-diagonal. Well-established time-stepping schemes are directly applicable.

Although only acoustic wave propagation in a waveguide has been addressed in this paper, the proposed technique is equally applicable to other systems which can be treated by the method of separation of variables, such as the circular cavity or the spherical cavity. More general homogeneous problems can thus be treated by introducing straight, circular or spherical boundaries. Further work related to extending the proposed technique to more general geometries and inhomogeneous problems is in progress. Half-space or full-space problems, where the artificial boundary has corners, can be modelled using the scaled boundary finite element method. The doubly asymptotic solution of the matrix-valued scaled boundary finite element equation in impedance is the subject of current research.

ACKNOWLEDGEMENTS

Carolin Birk performed some of the research reported herein during her visit to The University of New South Wales within the scope of a Marie Curie International Outgoing Fellowship for Career Development of the European Union. The financial support provided by the European Union and her appointment as a Visiting Fellow in the School of Civil and Environmental Engineering, The University of New South Wales, are gratefully acknowledged.

REFERENCES

- [1] Max Gunzburger Alvin Bayliss and Eli Turkel. Boundary conditions for the numerical solution of elliptic equations in exterior regions. *SIAM Journal of Applied Mathematics*, 42:430–451, 1982.
- [2] R. J. Astley. Infinite elements for wave problems: a review of current formulations and an assessment of accuracy. *International Journal for Numerical Methods in Engineering*, 49:951–976, 2000.
- [3] Mohammad Hossein Bazayari and Chongmin Song. A continued-fraction based high-order transmitting boundary for wave propagation in unbounded domains of arbitrary geometry. *International Journal for Numerical Methods in Engineering*, 74:209–237, 2008.
- [4] Dimitri E. Beskos. Boundary element methods in dynamic analysis. *Applied Mechanics Reviews*, 40:1–23, 1987.
- [5] Dimitri E. Beskos. Boundary element methods in dynamic analysis: Part II (1986–1996). *Applied Mechanics Reviews*, 50:149–197, 1997.
- [6] Bjorn Engquist and Andrew Majda. Radiation boundary conditions for acoustic and elastic wave calculations. *Communications on Pure and Applied Mathematics*, 32: 313–357, 1979.
- [7] Thomas L. Geers. Single and doubly asymptotic computational boundaries. In *IUTAM Symposium on Computational Methods for Unbounded Domains*, pages 135–141. Kluwer Academic Publishers, 1998.
- [8] Thomas L. Geers and Brett A. Lewis. Doubly asymptotic approximations for transient elastodynamics. *International Journal of Solids and Structures*, 34:1293–1305, 1997.
- [9] Thomas L. Geers and Brady J. Toothaker. Third-order doubly asymptotic approximations for computational acoustics. *Journal of Computational Acoustics*, 8:101–120, 2000.
- [10] Dan Givoli. High-order local non-reflecting boundary conditions: a review. *Wave Motion*, 39:319–326, 2004.
- [11] Dan Givoli. Non-reflecting boundary conditions. *Journal of Computational Physics*, 94:1–29, 1991.
- [12] Dan Givoli and Beny Neta. High-order non-reflecting boundary scheme for time-dependent waves. *Journal of Computational Physics*, 186:24–46, 2003.
- [13] Marcus J. Grote and Joseph B. Keller. Exact nonreflecting boundary condition for elastic waves. *SIAM Journal of Applied Mathematics*, 60:803–819, 2000.
- [14] Murthy N. Guddati and John L. Tassoulas. Continued-fraction absorbing boundary conditions for the wave equation. *Journal of Computational Acoustics*, 8(1):139–156, 2000.
- [15] Thomas Hagstrom and S. I. Hariharan. A formulation of asymptotic and exact boundary conditions using local operators. *Applied Numerical Mathematics*, 27:403–416, 1998.
- [16] Thomas Hagstrom and Timothy Warburton. A new auxiliary variable formulation of high-order local radiation boundary conditions: corner compatibility conditions and extensions to first-order systems. *Wave Motion*, 39:327–338, 2004.
- [17] Thomas Hagstrom, Assaf Mar-Or, and Dan Givoli. High-order local absorbing boundary conditions for the waves equation: Extensions and improvements. *Journal of Computational Physics*, 227:3322–3357, 2008.
- [18] Robert L. Higdon. Absorbing boundary conditions for difference approximations to the multi-dimensional wave equation. *Mathematics of Computation*, 47(176):437–459, 1986.
- [19] Eduardo Kausel. Local transmitting boundaries. *Journal of Engineering Mechanics*, 114(6):1011–1027, 1988.
- [20] Eduardo Kausel. Thin-layer method: formulation in the time domain. *International Journal for Numerical Methods in Engineering*, 37:927–941, 1994.
- [21] Steen Krenk. Unified formulation of radiation conditions for the wave equation. *International Journal for Numerical Methods in Engineering*, 53:275–295, 2002.
- [22] Z. P. Liao and H. L. Wong. A transmitting boundary for the numerical simulation of elastic wave propagation. *Soil Dynamics and Earthquake Engineering*, 3:174–183, 1984.
- [23] John Lysmer and Roger L. Kuhlemeyer. Finite dynamic model for infinite media. *Journal of the Engineering Mechanics Division*, 95(EM4):859–877, 1969.
- [24] Suriyon Prempramote, Chongmin Song, Francis Tin-Loi, and Gao Lin. High-order doubly asymptotic open boundaries for scalar wave equation. *International Journal for Numerical Methods in Engineering*, 29:340–374, 2009.
- [25] Warwick D. Smith. A nonreflecting plane boundary for wave propagation problems. *Journal of Computational Physics*, 15:492–503, 1974.
- [26] Chongmin Song and John P. Wolf. The scaled boundary finite-element method – alias consistent infinitesimal finite-element cell method – for elastodynamics. *Computer Methods in Applied Mechanics and Engineering*, 147:329–355, 1997.
- [27] Lonny L. Thompson, Runnong Huan, and Dantong He. Accurate radiation boundary conditions for the two-dimensional wave equation on unbounded domains. *Computer Methods in Applied Mechanics and Engineering*, 191:311–351, 2001.
- [28] Semyon V. Tsynkov. Numerical solution of problems on unbounded domains. A review. *Applied Numerical Mathematics*, 27:465–532, 1998.
- [29] Philip Underwood and T. L. Geers. Doubly asymptotic boundary-element analysis of dynamic soil–structure interaction. *International Journal of Solids and Structures*, 17:687–697, 1981.
- [30] John P. Wolf. *The scaled boundary finite element method*. Wiley & Sons, Chichester, 2003.